lubricants

MDPI

Article

Molecular Dynamics Simulation and Experimental Study of Friction and Wear Characteristics of Carbon Nanotube-Reinforced Nitrile Butadiene Rubber

Ce Liang [1,2,*], Changgeng Shuai [1,2] and Xin Wang [1,2]

[1] Institute of Noise & Vibration, Naval University of Engineering, Wuhan 430033, China
[2] Key Laboratory of Ship Vibration & Noise, Wuhan 430033, China
* Correspondence: 19100201@nue.edu.cn

Abstract: Nitrile butadiene rubber (NBR) and its various composite materials are widely employed as friction materials in mechanical equipment. The use of carbon nanotube (CNT) reinforcement in NBR for improved friction and wear characteristics has become a major research focus. However, the mechanisms underlying the improvement in the friction and wear characteristics of NBR with different CNT contents remain insufficiently elucidated. Therefore, we conducted a combined analysis of NBR reinforced with varying CNT contents through molecular dynamics (MD) simulations and ring–block friction experiments. The aim is to analyze the extent to which CNTs enhance the water-lubricated friction and dry wear properties of NBR and explore the improvement mechanisms through molecular chain characteristics. The results of this study demonstrate that as the mass fraction of CNTs (0%, 1.25%, 2.5%, 5%) increases, the water-lubricated friction coefficient of NBR continuously decreases. Under water-lubricated conditions, CNTs improve the water storage capacity of the NBR surface and enhance lubrication efficiency. In the dry wear state, CNTs help reduce scratch depth and dry wear volume.

Keywords: CNT/NBR composites; molecular dynamics; water-lubricated friction; dry wear

check for updates

Citation: Liang, C.; Shuai, C.; Wang, X. Molecular Dynamics Simulation and Experimental Study of Friction and Wear Characteristics of Carbon Nanotube-Reinforced Nitrile Butadiene Rubber. *Lubricants* **2024**, *12*, 261. https://doi.org/10.3390/lubricants12070261

Received: 2 July 2024
Revised: 18 July 2024
Accepted: 20 July 2024
Published: 22 July 2024

Copyright: © 2024 by the authors. Licensee MDPI, Basel, Switzerland. This article is an open access article distributed under the terms and conditions of the Creative Commons Attribution (CC BY) license (https://creativecommons.org/licenses/by/4.0/).

1. Introduction

NBR exhibits excellent mechanical properties, aging resistance, heat resistance, electrical insulation, and abrasion resistance, making it widely employed in mechanical industries for items such as seals and water-lubricated bearings [1–4]. In order to further enhance the friction and wear resistance of NBR, various fillers such as CNTs, graphene, alumina, silica, and carbon black have been utilized to modify nitrile rubber composite materials [5–9]. Both the type and content of the filler have an impact on the friction and wear properties of rubber; thus, a thorough analysis of the influencing mechanisms is crucial for the modification of rubber materials.

Since their discovery in 1991 [10], CNTs have been recognized as ideal fillers to improve polymer friction and wear properties due to their excellent mechanical properties, self-lubrication, and high wear resistance [11–13]. Ball-on-disc experiments have shown that the incorporation of CNTs at varying contents can increase the cross-linking density of rubber and reduce the friction coefficient [14]. Furthermore, within a certain range of proportions, a higher content of CNTs leads to a more significant decrease in the friction coefficient and enhanced wear resistance of NBR [15]. For marine stern-bearing base materials, the friction characteristics of NBR in water-lubricated environments and its anti-wear properties under harsh lubrication conditions are also crucial. Friction tests on ship stern bearings have demonstrated that CNT reinforcement can improve the mechanical properties and self-lubricating effect of NBR, thereby reducing the water-lubricated friction coefficient [16]. Comparative experiments between CNT-reinforced and graphene-reinforced NBR have shown that both carbon fillers effectively reduce the water-lubricated friction coefficient.

Compared to graphene, CNTs exhibit superior performance in reducing surface cracks and enhancing the wear resistance of NBR [17]. In addition, carbon-based materials such as CNTs and graphene have been shown to also reduce the coefficient of friction and the wear rate of metal composites due to good self-lubrication and excellent mechanical properties [18,19]. Although experimental methods can confirm the effectiveness of CNTs in improving friction and wear resistance, explaining the underlying mechanisms remains challenging. Furthermore, exploring the degree of improvement with different contents of carbon nanotubes through repetitive experiments is inefficient.

In recent years, with the rapid development of computer hardware performance, the use of molecular dynamics (MD) methods to simulate the friction and wear performance of NBR composite materials at the nanoscale has become a research focus [20–23]. Y. Li et al. [24] utilized MD simulations to investigate the atomic motion in the contact friction zone between iron atoms and CNT-reinforced NBR. The simulation results showed that the addition of CNTs increased the shear modulus of the composite material by up to 60% and significantly improved its friction performance. Building on these findings, Y. Li et al. simulated the friction and anti-wear properties of defect CNTs and functionalized CNTs in NBR composite materials [25–27]. Furthermore, the effects of different contents and lengths of CNTs, as well as different acrylonitrile contents, on the friction characteristics of NBR can also be analyzed through molecular simulations [28,29]. Molecular simulations provide a theoretical framework at the nano-scale, aiding in the simulation of friction and anti-wear properties and thereby increasing understanding of the mechanisms of friction performance improvement. In addition to molecular simulations, data-driven approaches such as machine learning are also of great interest for analyzing and predicting the friction characteristics of carbon-reinforced composites [30,31]. Nano-scale simulation results can also assist in predicting macroscopic friction and wear characteristics.

Therefore, in this study, the frictional and wear processes of CNT-reinforced NBR were modeled using a molecular dynamics approach. The micro-mechanisms of the reductions in the water-lubricated friction coefficient and the dry wear rate were analyzed through the frictional wear process at the molecular level. Macroscopic friction and wear experiments were also conducted to verify the degree of improvement in the friction and wear characteristics of NBR with different mass fractions (0%, 1.25%, 2.5%, and 5%) of CNTs. Considering that a too-high CNT mass fraction would lead to unsatisfactory dispersion in the rubber matrix [32,33], the CNT mass fraction in this study does not exceed 5%. Both the molecular simulation and macroscopic experimental results showed that the water-lubricated friction coefficients and the dry wear rates of the NBR composites decreased continuously with increased CNT content. This study provides valuable insights into the friction enhancement mechanism and degree of improvement of carbon-based fillers in polymers.

2. Materials and Methods

2.1. MD Simulations Modeling and Methods

This study employed Materials Studio (MS 2019) for model construction and utilized the Large-scale Atomic/Molecular Massively Parallel Simulator (LAMMPS) for system optimization and MD simulations [34]. The Consistent Valence Force Field has been applied in previous mechanical and friction simulations of carbon-reinforced nitrile rubber [35,36], and was employed in this study for simulation purposes. First, pure NBR is molecularly modeled. NBR is a copolymer composed of acrylonitrile and butadiene monomers. In this simulation, the NBR polymer chains are constructed based on a 1:1 ratio of butadiene and acrylonitrile monomers. The polymerization degree of the NBR chains is set to 20. A periodic box with dimensions of 50 Å × 30 Å × 30 Å is constructed in the MS software. Using the Monte Carlo method [37], multiple NBR polymer chains are placed in the periodic box until the box density reaches the actual density of NBR, which is 1.0 g/cm^3. The constructed pure NBR unit cell is shown in Figure 1a. This is followed by the modeling of the CNT/NBR RVE. An armchair single-walled CNT is placed in the center of

a 50 Å × 30 Å × 30 Å periodic box, such that the axial direction of the CNT is parallel to the x-direction of the box. The Monte Carlo method is used to fill three boxes with NBR molecular chains, to achieve the CNT mass fractions of 1.25%, 2.5%, and 5%. The structure and size of the CNTs and the 5% mass fraction CNT/NBR filling process are shown in Figure 1b.

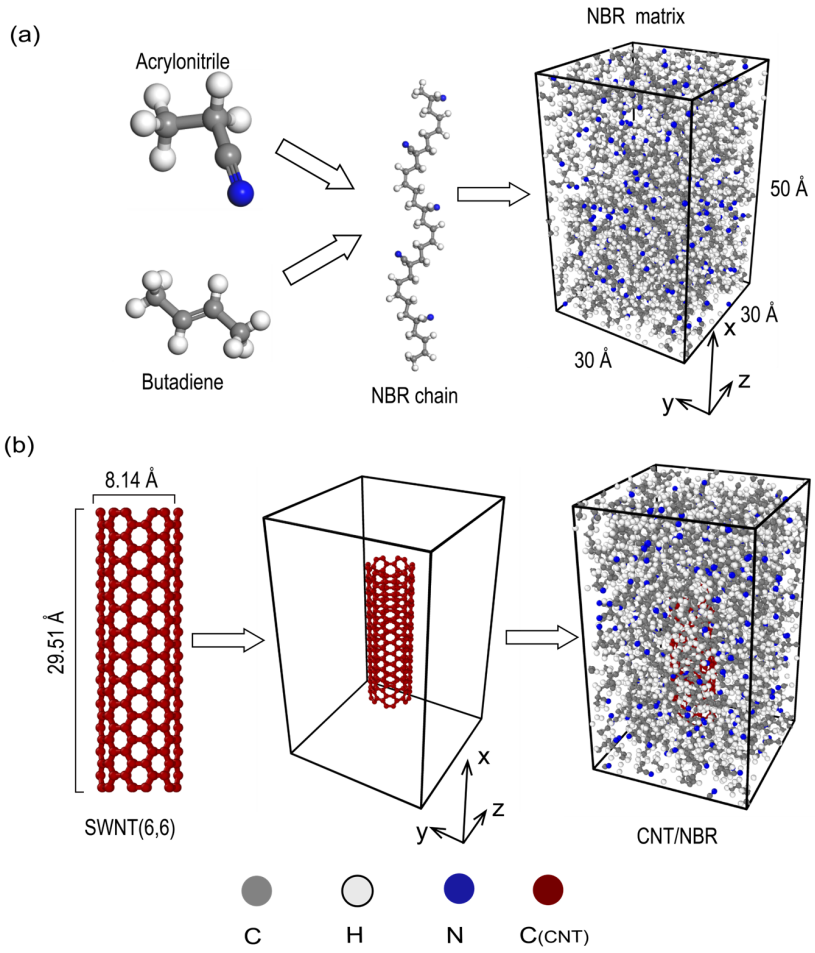


Figure 1. Construction of MD model—(**a**) NBR matrix; (**b**) CNT/NBR.

After model construction, the pure NBR and CNT/NBR RVE periodic unit cells were imported into LAMMPS using the msi2lmp module in the MS software for system optimization and simulation. The initially established amorphous unit cell had high total energy and exhibited highly unstable internal states. To achieve energy minimization, the conjugate gradient method was applied to the entire molecular system. The energy convergence threshold was set to 10^{-5} kcal/mol, and the force convergence criterion was set to 10^{-4} kcal/mol/Å. To eliminate peculiar connections between polymer chains and molecules, a 1 ns molecular dynamics equilibration was performed on the NPT (constant pressure, constant temperature) ensemble at a temperature of 300 K and a pressure of 0.1 MPa (atmospheric pressure). Subsequently, the equilibrated unit cell was subjected to an annealing process with a temperature range of 250 K to 500 K and a temperature step size of 50 K, repeated for 10 cycles. The repeated high-temperature to low-temperature annealing cycles allowed for better relaxation and optimization of the molecular structure within the system. A subsequent 1 ns molecular dynamics equilibration was performed on the NVT (canonical ensemble) ensemble. The optimized total energy of the system reached its lowest level at a temperature of 300 K, and the pressures in all directions were reduced to zero.

Taking into consideration the context of NBR materials' application as friction materials for water-lubricated bearings, a molecular simulation of NBR's frictional properties was conducted using water molecules as the lubricating medium and copper (Cu) as the corresponding material for frictional contact. As depicted in Figure 2a, the 7-layer close-packed Cu(1 1 1) was placed on top of a pure NBR box. The bottom 5 Å region of the nitrile rubber box was fixed as the fixed layer, while the remaining portion served as the sliding layer. There were a total of 3451 copper atoms and 250 water molecules. A normal pressure level of 0.5 MPa (7.5×10^{-12} N) was applied to the copper atomic layer, along with a tangential sliding velocity of 0.0055 Å/ps (0.55 m/s) to simulate water-lubricated frictional motion. The frictional force was equal to the total tangential force on all copper atoms. The coefficient of friction is the ratio of the friction force to the normal force. Throughout the simulation process, the copper atomic layer traveled a distance of 100 Å, with a time step of 1 fs. The average value of the friction coefficient in a stable state after 150 ps was considered as the effective value. The water-lubricated friction process for 5% mass fraction CNT/NBR is illustrated in Figure 2b.

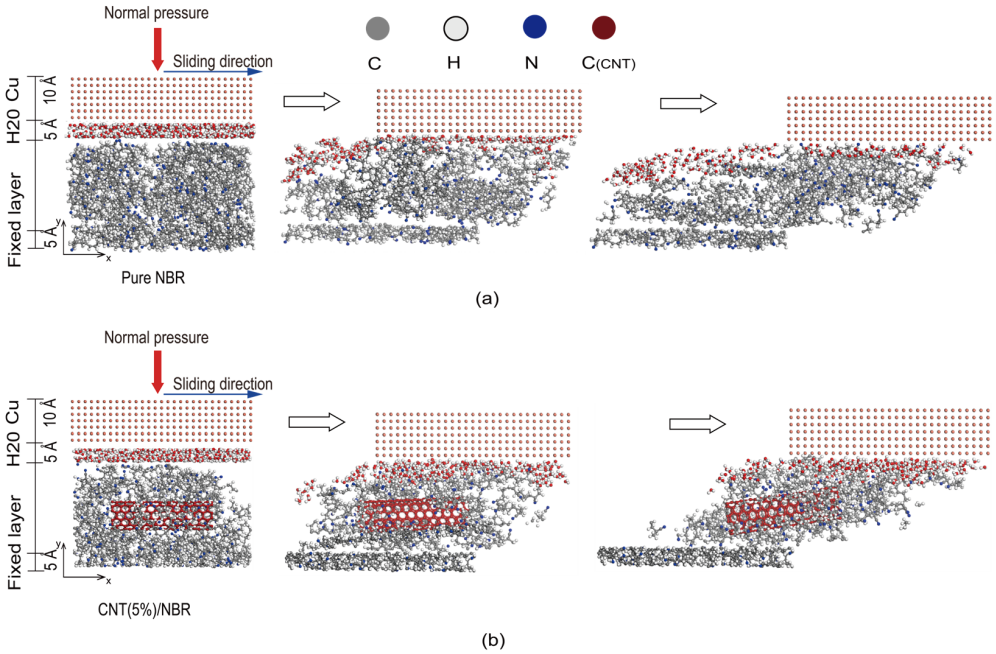


Figure 2. Water-lubricated friction simulation process—(**a**) pure NBR; (**b**) 5% CNT/NBR.

To predict the wear states of NBR composite materials under adverse lubrication conditions, a molecular simulation of wear characteristics was conducted in a dry friction environment, with copper chosen as the frictional counterpart. As illustrated in the figure, the 7-layer close-packed Cu(1 1 1) was placed on top of a pure nitrile rubber box. There were a total of 3451 copper atoms. The bottom 5 Å region of the nitrile rubber box was fixed as the stationary layer, while the remaining portion served as the sliding layer. A normal pressure level of 0.5 MPa (7.5×10^{-12} N) was applied to the copper atomic layer, along with a tangential sliding velocity of 0.0257 Å/ps (2.57 m/s) to simulate dry frictional wear motion. Throughout the simulation process, the copper atomic layer traveled a distance of 100 Å, with a time step of 1 fs. Molecular wear was characterized by the proportion of atoms and molecules that detached from the polymer molecular chains over the entire frictional motion process. The dry wear process for 5% mass fraction CNT/NBR is illustrated in Figure 3b.

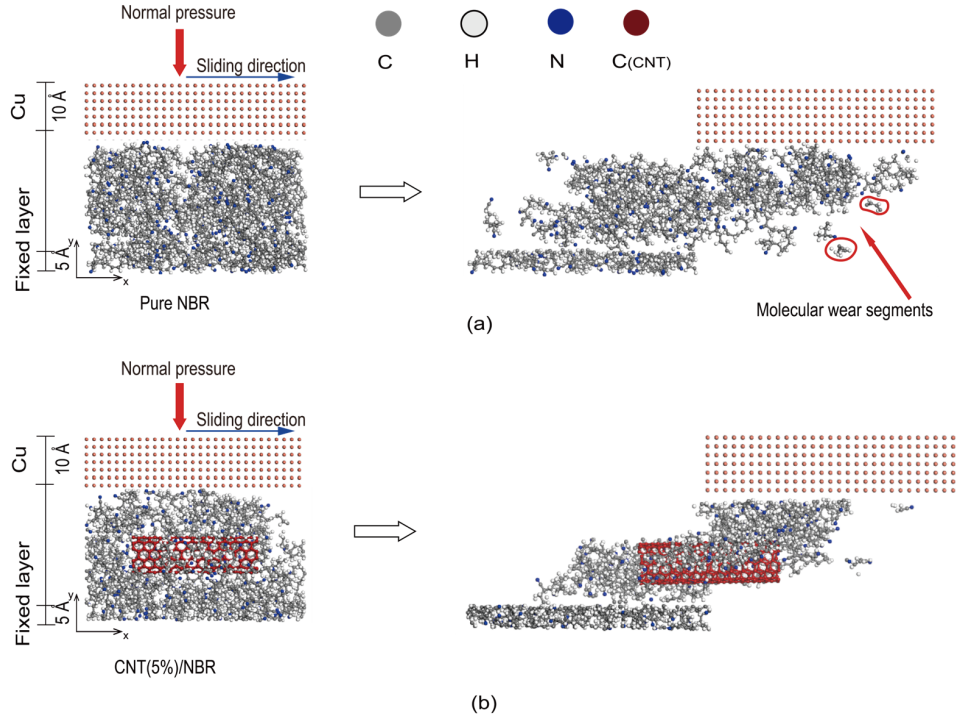


Figure 3. Dry wear simulation process—(**a**) pure NBR; (**b**) 5% CNT/NBR.

2.2. Materials and Experimental Setup

Four types of CNT/NBR composite materials, with mass fractions of 0% (pure NBR), 1.25%, 2.5%, and 5%, were prepared. The CNT was a single-wall CNT manufactured by TANFENG Technology (Suzhou, China), Model No. TF-22011 (carbon nanotubes are 5–20 μm in length and 1–2 nm in diameter). The CNT/NBR composite materials were fabricated by physically blending CNTs with the NBR. CNTs were homogeneously filled into the natural rubber (NR) during the compounding process and fully roll-mixed. The complete preparation process of CNT/NBR is shown in Figure 4.

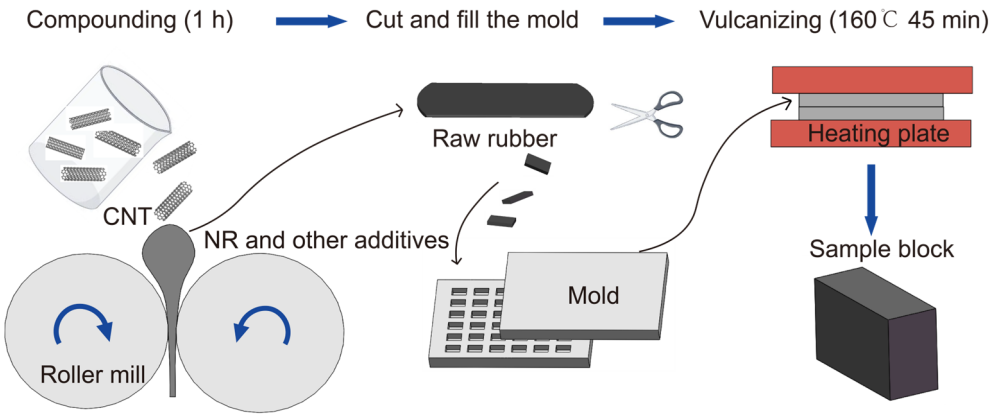


Figure 4. CNT/NBR preparation process.

The CNT/NBR composites studied in this work will be used as the friction side material of marine water-lubricated bearings. In order to correspond to the friction structure of the bearings, we used the ring–block friction pair for the experiments. The material of the friction side corresponding to the CNT/NBR specimen block was copper alloy (consistent with the paired side of the marine water-lubricated bearing). Friction performance testing of the ring–block under water lubrication was conducted using a UMT-type friction tester manufactured by the Bruker Corporation (Billerica, MA, USA), as depicted in Figure 5a. A

normal pressure level of 0.5 MPa was applied by the motor, with the copper ring rotating at 300 rpm (0.55 m/s). The pressure and speed were set to simulate the actual operating conditions of a water-lubricated bearing. The coefficient of friction can be stabilized and sustained within 30 s, according to pre-tests. Therefore, we tested each sample for two minutes and took the average coefficient of friction during one minute of the stabilization phase as a representative value.

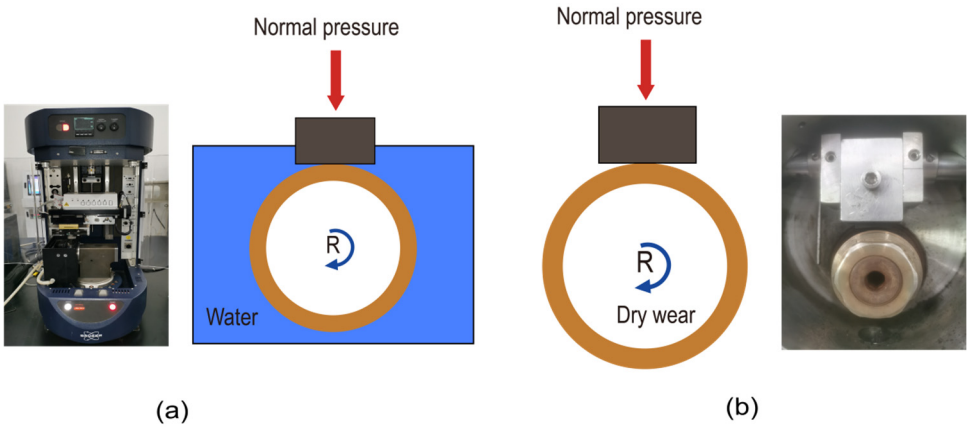


Figure 5. Ring–block friction structure and testing machine—(**a**) water-lubricated; (**b**) dry wear.

Dry friction wear testing was conducted using an MRH-3G friction and wear tester manufactured by Hengxu Corporation (Jinan, China), as shown in Figure 5b. A normal pressure level of 0.5 MPa was applied, with the copper ring rotating at 1000 rpm (2.57 m/s). The testing lasted for 2 h, and wear was characterized by the ratio of weight loss and volume loss of the sample block before and after wear. The dimensions of the copper ring and sample block used in both water-lubricated friction testing and dry wear testing are provided in Table 1.

Table 1. Structural parameters of copper ring and sample block.

	Structure Component	Parameter Description	Value [mm]
Water-lubricated friction test	Copper ring	Outer diameter	35
		Inner diameter	28
	CNT/NBR block	Thickness	10
		Length	16.5
		Height	10
		Thickness	6.5
Dry wear test	Copper ring	Outer diameter	49
		Inner diameter	42
	CNT/NBR block	Thickness	12.3
		Length	19.2
		Height	12.3
		Thickness	12.3

3. Results and Discussion

3.1. Water-Lubricated Friction Chracteristics

Figure 6 presents the water-lubricated friction coefficient results obtained from MD simulations and ring–block friction–wear experiments. Numerically, both the MD simulations and macroscopic experiments demonstrate that the incorporation of CNTs effectively reduces the water-lubricated friction coefficient of NBR. Within the mass fraction range of 0–5%, an increase in CNT content correlates with a more pronounced improvement in the frictional performance of NBR. Both the MD simulations and the ring–block friction–wear

experiments exhibit consistency in this trend. The simulations indicate that the friction coefficient of 5% CNT/NBR, the sample with the highest CNT content, is reduced by 57.6% compared to pure NBR, while the experiments show a reduction of 60.8%. The simulation results in Figure 6 demonstrate that, in addition to reducing the friction coefficient values, the incorporation of CNTs decreases the amplitude of NBR friction coefficient fluctuations. This reduction in friction coefficient fluctuations corresponds to an improvement in the "stick-slip" phenomenon.

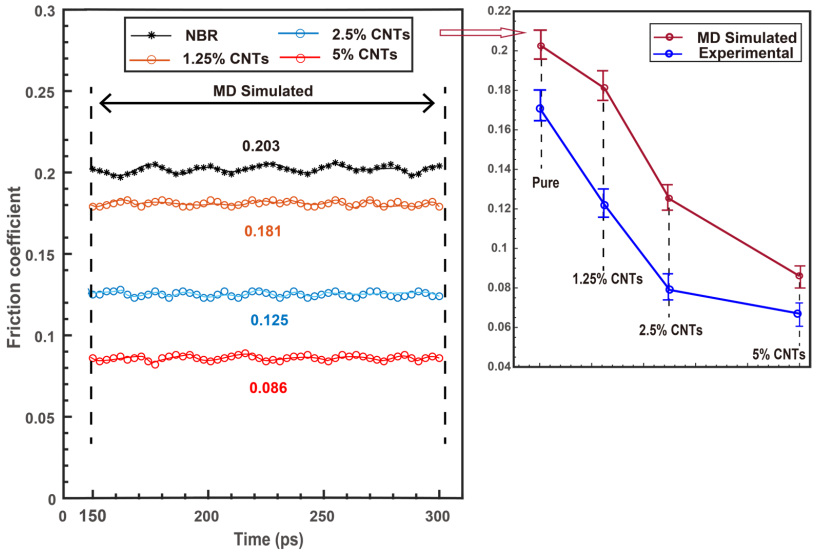


Figure 6. Simulated and experimental results of water-lubricated friction properties. (Error bars mean standard deviation).

Analyzing the improvement mechanism of this frictional characteristic from a molecular perspective reveals that upon the addition of CNTs, enhanced by strong van der Waals forces [32], more NBR polymer chains aggregate around the CNTs, resulting in a tighter cross-linking structure. Within a certain range of mass fractions, higher CNT content leads to a more pronounced van der Waals interaction between CNTs and NBR polymer chains. The close aggregation of NBR polymer chains around CNTs reduces the intermolecular forces between NBR and the metal counterpart molecules during the friction process. This weakening of adhesive effects at the contact interface subsequently decreases the tangential resistance at the contact interface, resulting in a reduction in the friction coefficient. Simultaneously, the weakened adhesive effects alleviate the "stick-slip" phenomenon during sliding. Observations of the friction specimens' SEM images are depicted in Figure 7, illustrating typical SEM images of 5% CNT/NBR friction specimens. From Figure 7, it can be observed that NBR rubber chains are closely attached around the CNTs. Additionally, the cross-linking degree of NBR in the CNT/NBR specimens appears denser compared to that of pure NBR. These observed phenomena align well with the molecular simulation process, further validating the mechanism by which CNT incorporation modifies NBR friction characteristics.

Furthermore, insights are provided from the perspectives of lubrication and material hydrophilicity, as illustrated in Figure 8. From the water-lubricated molecular simulation process, it is evident that the inclusion of CNTs leads to a greater retention of water molecules at the friction interface, enhancing lubrication. This is attributed to the closer aggregation of NBR around the CNTs, which creates more space at the interface to store water molecules. The increased presence of water molecules serves to further improve the water-lubricated friction characteristics of NBR. Results from hydrophilicity tests demonstrate that as the mass fraction of carbon nanotubes increases to 5%, the water contact angle of the composite material decreases from 92.2° to 80.6°. The improvement in hydrophilicity also signifies the superior water retention capabilities of CNT/NBR, aligning well with

the molecular simulation. Enhanced lubrication and hydrophilicity further accentuate the improvement effects of CNTs on the water-lubricated friction characteristics of NBR. In addition, it is well known that the self-lubricating property of CNTs can also reduce the friction coefficients of composites.

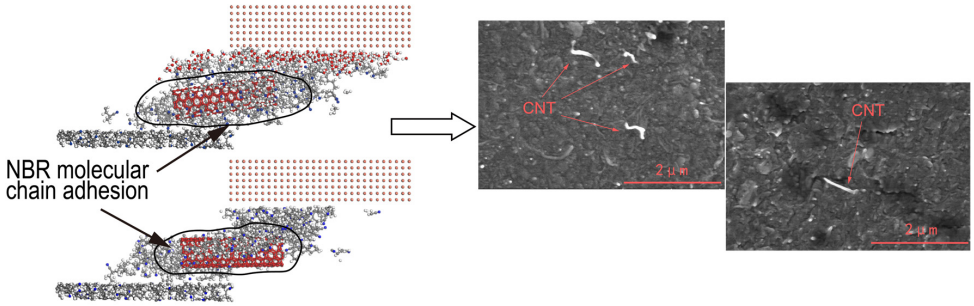


Figure 7. SEM images of 5% CNT/NBR.

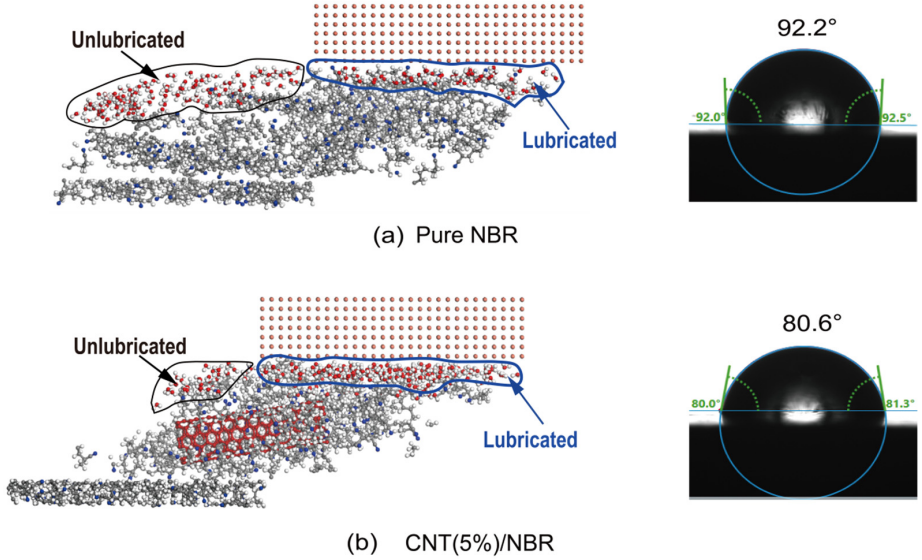


Figure 8. Water molecule storage and hydrophilicity of (**a**) NBR; (**b**) 5% CNT/NBR.

3.2. Dry Wear Characteristics

The wear volume statistics from the molecular simulations and dry wear experiments are presented in Figure 9. In molecular simulations, the wear volume is characterized based on the fragmentation of polymer molecules and atomic fragments during the wear process. Experimental wear volume is quantified by scanning the surface of the sample block using confocal laser microscopy after wear. As depicted in Figure 9, both the molecular wear rate and the experimental wear volume decrease continuously with the increase in CNT mass fraction. This decreasing trend in wear volume aligns well with the results of the molecular dynamics simulations. The molecular wear rate decreases from 11.5% to 6.7%, while the wear volume of the sample block reduces from 1.76×10^{10} μm^3 to 0.28×10^{10} μm^3.

Analyzing the mechanism behind the improvement of dry wear characteristics from a molecular perspective reveals insights similar to those observed in the water-lubricated friction simulations. As depicted in Figure 7, the powerful van der Waals forces led to the tight aggregation of NBR polymer chains around the CNTs. The higher degree of cross-linking and the proximity of NBR chains to CNTs reduced the adhesive effects of NBR at the contact interface, consequently lowering the extent of wear. Moreover, the denser NBR polymer chains also contributed to the reduction in crack growth and extension during the wear process, resulting in decreased wear volume.

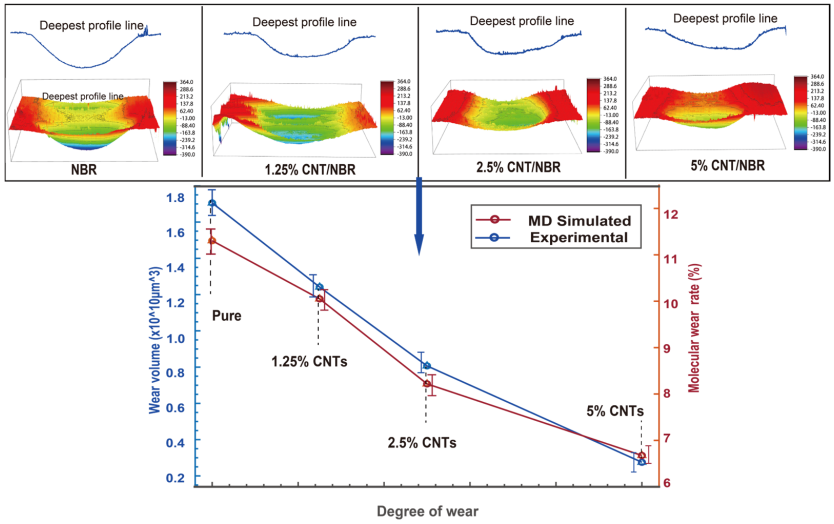


Figure 9. Dry wear simulation and experimental results. (Error bars mean standard deviation).

Furthermore, we conducted observations of the worn surface morphology of each specimen. In Figure 10, typical wear morphologies of pure NBR and 5% CNT/NBR composites are presented. From Figure 10, it is evident that after dry wear, both pure NBR and 5% CNT-NBR composites exhibit pronounced plow grooves on their surface. Additionally, there are noticeable signs of wear and detachment on the surface of pure NBR. Measurements of local wear traces reveal that the scratch depth of pure NBR is deeper compared to that of 5% CNT-NBR. The maximum scratch depth in NBR is 113.7 μm deeper than in 5% CNT-NBR, further indicating the enhancement of abrasion resistance in NBR composites with the incorporation of CNTs.

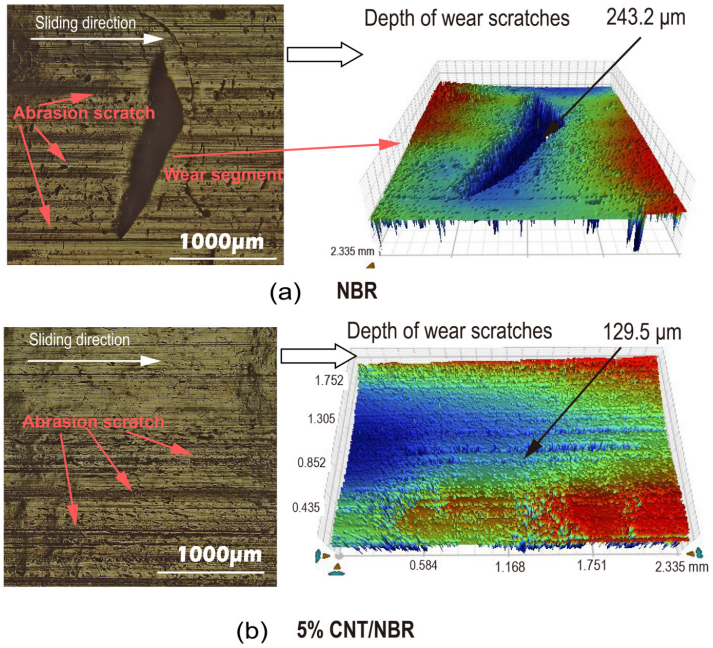


Figure 10. Typical wear surface morphology of (**a**) NBR; (**b**) 5% CNT/NBR.

4. Conclusions

This study combines molecular dynamics simulations and ring–block friction–wear experiments to comprehensively analyze the friction and wear characteristics of CNT-reinforced NBR. A comparative analysis of the water-lubricated friction characteristics and dry wear properties of CNT-reinforced NBR at different mass fractions (0%, 1.25%,

2.5%, 5%) was conducted. The possible agglomeration of higher mass fractions of carbon nanotubes in NBR needs to be further analyzed in future research. The mechanism of CNTs for improving the friction and wear characteristics of NBR has been comprehensively explored at the molecular chain scale and the macroscopic scale. Both the simulation and experimental results consistently demonstrate that with increases in the mass fraction of CNTs, the water-lubricated friction characteristics and wear resistance of NBR continuously improve. The incorporation of CNTs leads to higher cross-linking density of NBR polymer chains and their tighter aggregation around CNTs. This change in CNT/NBR molecular chains mitigates adhesive phenomena at the contact interface, thereby reducing frictional shear forces. Under water-lubricated conditions, the presence of CNTs results in more water molecules being stored at the friction interface, accompanied by an enhancement in material hydrophilicity, thereby optimizing lubrication efficiency. In dry wear conditions, the denser molecular chains alleviate material crack propagation and extension. Moreover, the excellent anti-wear properties of CNTs at the wear interface reduce the wear volume of nitrile rubber. By integrating multidimensional analyses at the molecular and macroscopic levels, this study contributes to a more comprehensive understanding of the mechanisms by which CNTs improve the friction and wear properties of NBR.

Author Contributions: Conceptualization, C.S.; Methodology, C.L.; Validation, X.W.; Formal analysis, X.W.; Investigation, C.S.; Resources, C.S.; Writing—original draft, C.L.; Writing—review & editing, X.W.; Visualization, C.L.; Project administration, X.W. All authors have read and agreed to the published version of the manuscript.

Funding: This research was funded by the Defense Foundation Enhancement Program, grant number [2020-XXJQ-ZD-20X].

Data Availability Statement: The data that support the findings of this study are available from the corresponding author upon reasonable request.

Conflicts of Interest: The authors declare no conflict of interest.

References

1. Akhmedgoraeva, A.R.; Sultanov, A.A.; Galimzyanova, R.Y.; Khakimullin, Y.N. Nonhardening Sealants Based on Modified Nitrile Butadiene Rubber. *Polym. Sci. Ser. D* **2022**, *15*, 379–383. [CrossRef]
2. Porter, C.; Zaman, B.; Pazur, R. A Critical Examination of the Shelf Life of Nitrile Rubber O-Rings Used in Aerospace Sealing Applications. *Polym. Degrad. Stab.* **2022**, *206*, 110199. [CrossRef]
3. Zhou, G.; Wu, K.; Pu, W.; Li, P.; Han, Y. Tribological Modification of Hydrogenated Nitrile Rubber Nanocomposites for Water-Lubricated Bearing of Ship Stern Shaft. *Wear* **2022**, *504–505*, 204432. [CrossRef]
4. Jin, D.; Xiao, K.; Han, Y.; Xiang, G.; Zhou, Z.; Wang, J. A Preparation Method of Porous Surface Nitrile Butadiene Rubber with Low Friction Coefficient under Water Lubrication Condition by Salt Leaching. *J. Appl. Polym. Sci.* **2021**, *138*, 50555. [CrossRef]
5. Guezzout, Z.; Boublia, A.; Haddaoui, N. Enhancing Thermal and Mechanical Properties of Polypropylene-Nitrile Butadiene Rubber Nanocomposites through Graphene Oxide Functionalization. *J. Polym. Res.* **2023**, *30*, 207. [CrossRef]
6. Alhareb, A.; Akil, H.; Ahmad, Z. Poly(Methyl Methacrylate) Denture Base Composites Enhancement by Various Combinations of Nitrile Butadiene Rubber/Treated Ceramic Fillers. *J. Thermoplast. Compos. Mater.* **2017**, *30*, 1069–1090. [CrossRef]
7. Hussain, M.; Yasin, S.; Ali, A.; Li, Z.; Fan, X.; Song, Y.; Zheng, Q.; Wang, W. Synergistic Impact of Ionic Liquid on Interfacial Interaction and Viscoelastic Behaviors of Silica Filled Nitrile Butadiene Rubber Nanocomposites. *Compos. Part. A Appl. Sci. Manuf.* **2022**, *163*, 107202. [CrossRef]
8. Zainal Abidin, Z.; Mamauod, S.N.L.; Romli, A.Z.; Sarkawi, S.S.; Zainal, N.H. Synergistic Effect of Partial Replacement of Carbon Black by Palm Kernel Shell Biochar in Carboxylated Nitrile Butadiene Rubber Composites. *Polymers* **2023**, *15*, 943. [CrossRef]
9. Li, X.; Li, Y.; Qian, C.; Zhao, J.; Wang, S. Molecular Dynamics Study of the Mechanical and Tribological Properties of Graphene Oxide-Reinforced Polyamide 66/Nitrile Butadiene Rubber Composites. *Appl. Phys. A* **2023**, *129*, 276. [CrossRef]
10. Iijima, S. Helical Microtubules of Graphitic Carbon. *Nature* **1991**, *354*, 56–58. [CrossRef]
11. Ruoff, R.S.; Lorents, D.C. Mechanical and Thermal Properties of Carbon Nanotubes. *Carbon* **1995**, *33*, 925–930. [CrossRef]
12. Makowiec, M.E.; Blanchet, T.A. Improved Wear Resistance of Nanotube- and Other Carbon-Filled PTFE Composites. *Wear* **2017**, *374–375*, 77–85. [CrossRef]
13. Zou, A.; Li, D. Effect of Carbon Nanotube on the Oscillating Wear Behaviour of Metal-PTFE Multilayer Composites. *J. Wuhan Univ. Technol. Mater. Sci.* **2018**, *33*, 1271–1274. [CrossRef]

14. Jansinak, S.; Markpin, T.; Wimolmala, E.; Mahathanabodee, S.; Sombatsompop, N. Tribological Properties of Carbon Nanotube as Co-Reinforcing Additive in Carbon Black/Acrylonitrile Butadiene Rubber Composites for Hydraulic Seal Applications. *J. Reinf. Plast. Compos.* **2018**, *37*, 1255–1266. [CrossRef]
15. Felhös, D.; Karger-Kocsis, J.; Xu, D. Tribological Testing of Peroxide Cured HNBR with Different MWCNT and Silica Contents under Dry Sliding and Rolling Conditions against Steel. *J. Appl. Polym. Sci.* **2008**, *108*, 2840–2851. [CrossRef]
16. Li, F.; Yang, X.; He, L.; Shuai, C.G. Friction Properties of Carbon Nanotubes Reinforced Nitrile Composites under Water Lubricated Condition. *AMR* **2011**, *284–286*, 611–614. [CrossRef]
17. Liu, X.; Huang, J.; Yang, C.; Wang, P.; Xing, S.; Zhong, D.; Zhou, X. Effects of Graphene and CNTs Reinforcement on the Friction Mechanism of Nitrile Butadiene Rubber under Water Lubrication Conditions. *Wear* **2022**, *500–501*, 204334. [CrossRef]
18. Dorri Moghadam, A.; Omrani, E.; Menezes, P.L.; Rohatgi, P.K. Mechanical and Tribological Properties of Self-Lubricating Metal Matrix Nanocomposites Reinforced by Carbon Nanotubes (CNTs) and Graphene—A Review. *Compos. Part. B Eng.* **2015**, *77*, 402–420. [CrossRef]
19. Omrani, E.; Moghadam, A.D.; Kasar, A.K.; Rohatgi, P.; Menezes, P.L. Tribological Performance of Graphite Nanoplatelets Reinforced Al and Al/Al2O3 Self-Lubricating Composites. *Materials* **2021**, *14*, 1183. [CrossRef]
20. Liu, X.; Zhou, X.; Kuang, F.; Zuo, H.; Huang, J. Mechanical and Tribological Properties of Nitrile Rubber Reinforced by Nano-SiO_2: Molecular Dynamics Simulation. *Tribol. Lett.* **2021**, *69*, 54. [CrossRef]
21. Liu, X.; Huang, J.; Yang, C.; Xing, S.; Wang, P.; Zhou, X. Molecular Dynamics Simulations Probing the Effects of Interfacial Interactions on the Tribological Properties of Nitrile Butadiene Rubber/Nano-SiO2 under Water Lubrication. *Mater. Today Commun.* **2022**, *32*, 104165. [CrossRef]
22. Cui, J.; Zhao, J.; Wang, S.; Li, Y. A Comparative Study on Enhancement of Mechanical and Tribological Properties of Nitrile Rubber Composites Reinforced by Different Functionalized Graphene Sheets: Molecular Dynamics Simulations. *Polym. Compos.* **2021**, *42*, 205–219. [CrossRef]
23. He, E.; Wang, S.; Tang, L.; Chen, J. A Study on the Enhancement of the Tribological Properties of Nitrile-Butadiene Rubber Reinforced by Nano-ZnO Particles from an Atomic View. *Mater. Res. Express* **2021**, *8*, 095009. [CrossRef]
24. Li, Y.; Wang, S.; Arash, B.; Wang, Q. A Study on Tribology of Nitrile-Butadiene Rubber Composites by Incorporation of Carbon Nanotubes: Molecular Dynamics Simulations. *Carbon* **2016**, *100*, 145–150. [CrossRef]
25. Wang, M.; Li, Y.; Qian, C.; Zhao, J.; Wang, S. Molecular Dynamics Simulations of Defective Carbon Nanotubes on the Aging and Friction Properties of Nitrile Butadiene Rubber Composites. *Polym. Compos.* **2023**, *44*, 1228–1239. [CrossRef]
26. Qian, C.; Li, Y.; Zhao, J.; Wang, S. Effect of Single-Vacancy- and Vacancy-Adsorbed-Atom-Defective CNTs on the Mechanical and Tribological Properties of NBR Composites: Molecular Dynamics Simulations. *J. Polym. Res.* **2023**, *30*, 99. [CrossRef]
27. Cui, J.; Zhao, J.; Wang, S.; Wang, Y.; Li, Y. Effects of Carbon Nanotubes Functionalization on Mechanical and Tribological Properties of Nitrile Rubber Nanocomposites: Molecular Dynamics Simulations. *Comput. Mater. Sci.* **2021**, *196*, 110556. [CrossRef]
28. Qian, C.; Li, Y.; Zhao, J.; Wang, S.; He, E. Thermal-oxidative Aging and Tribological Properties of Carbon Nanotube/Nitrile Butadiene Rubber Composites with Varying Acrylonitrile Content: Molecular Dynamics Simulations. *Polym. Eng. Sci.* **2023**, *63*, 1516–1527. [CrossRef]
29. Li, C.; Liu, Z.; Huo, Y.; Li, F.; Tang, L. Molecular Dynamics Simulation of Mechanical and Tribological Properties of Nitrile Butadiene Rubber with Different Length and Content Carbon Nanotubes. *Mater. Today Commun.* **2023**, *36*, 106693. [CrossRef]
30. Hasan, M.S.; Kordijazi, A.; Rohatgi, P.K.; Nosonovsky, M. Triboinformatic Modeling of Dry Friction and Wear of Aluminum Base Alloys Using Machine Learning Algorithms. *Tribol. Int.* **2021**, *161*, 107065. [CrossRef]
31. Hasan, M.S.; Kordijazi, A.; Rohatgi, P.K.; Nosonovsky, M. Machine Learning Models of the Transition from Solid to Liquid Lubricated Friction and Wear in Aluminum-Graphite Composites. *Tribol. Int.* **2022**, *165*, 107326. [CrossRef]
32. Ma, P.-C.; Siddiqui, N.A.; Marom, G.; Kim, J.-K. Dispersion and Functionalization of Carbon Nanotubes for Polymer-Based Nanocomposites: A Review. *Compos. Part A Appl. Sci. Manuf.* **2010**, *41*, 1345–1367. [CrossRef]
33. Thongkong, N.; Wisunthorn, S.; Pichaiyut, S.; Nakason, C.; Kiatkamjornwong, S. Natural Rubber Nanocomposites Based on Hybrid Filler of Zinc Nanoparticles and Carbon Nanotubes: Electrical Conductivity and Other Related Properties. *Express Polym. Lett.* **2020**, *14*, 1137–1154. [CrossRef]
34. Plimpton, S. Fast Parallel Algorithms for Short-Range Molecular Dynamics. *J. Comput. Phys.* **1995**, *117*, 1–19. [CrossRef]
35. Yang, B.; Wang, S.; Song, Z.; Liu, L.; Li, H.; Li, Y. Molecular Dynamics Study on the Reinforcing Effect of Incorporation of Graphene/Carbon Nanotubes on the Mechanical Properties of Swelling Rubber. *Polym. Test.* **2021**, *102*, 107337. [CrossRef]
36. Yang, B.; Li, Y.; Wang, S.; Nie, R.; Wang, Q. Aminosilane Modified Graphene Oxide for Reinforcing Nitrile Butadiene Rubber: Experiments and Molecular Dynamic Simulations. *Compos. Sci. Technol.* **2023**, *235*, 109956. [CrossRef]
37. Siepmann, J.I.; McDonald, I.R. Monte Carlo Simulations of Mixed Monolayers. *Mol. Phys.* **1992**, *75*, 255–259. [CrossRef]

Disclaimer/Publisher's Note: The statements, opinions and data contained in all publications are solely those of the individual author(s) and contributor(s) and not of MDPI and/or the editor(s). MDPI and/or the editor(s) disclaim responsibility for any injury to people or property resulting from any ideas, methods, instructions or products referred to in the content.